Michelson Interferometry with Keck 1

P. G. Tuthill, J. D. Monnier & W. C. Danchi

University of California Space Sciences Laboratory
MC 7450, Berkeley, CA, 94720-7450

C. A. Haniff

University of Cambridge, Cavendish Laboratory, Madingley Rd., Cambridge CB3 OHE, U.K.

ABSTRACT

We have used the technique of aperture masking to transform the 10m Keck telescope into a separate-element, multiple aperture Michelson interferometer. This has allowed a dramatic gain in signal-to-noise to be achieved as compared to conventional full-pupil interferometry for bright targets such as evolved giant and supergiant stars. Preliminary results from a program of near-infrared diffraction-limited imaging of such stars are presented. Multi-wavelength images in the infrared JHK and L bands have revealed complex and asymmetric morphologies in the inner dust shells surrounding a number of proto-typical dust-enshrouded IR stars. In addition, we have imaged the stellar photospheres of some of our largest target stars, allowing us to measure diameters and search for structure, such as giant convective cells, on the stellar surface.

Keywords: stars: imaging – stars: diameters – mass loss – stellar interferometry

1. INTRODUCTION

With a diameter of 10 m, the resolution afforded by the keck 1 telescope is well suited to the study of the nearest and brightest dust-enshrouded stars. In order to utilise the unique properties of the kecks to their best advantage, a number of years ago we initiated a program of aperture masking and Fourier synthesis imaging targeted at the study of bright evolved stars. Both theoretical and experimental studies have highlighted the gains in signal-to-noise ratio (SNR) made available by using sparse rather than filled apertures in interferometric observations of bright sources (Roddier 1988, Haniff & Buscher 1992). Our own results have have verified these predictions, and enabled us to reconstruct complex images at diffraction-limited angular resolution in the near-infrared.

Using multi-wavelength images spanning the infrared JHK and L bands, we have begun to address some of the most pressing questions related to the latest stages of stellar evolution, through observations of a number of the brightest Mira variables and evolved supergiants. Most importantly, we have been exploring the processes underlying mass loss, a key feature of such evolved systems. Although theoretical models usually assume spherical symmetry, there has been a growing body of evidence (e.g. from molecular and polarization data, spectrophotometry, and observations of planetary nebulae) that mass loss is often anisotropic. Our high-resolution images have provided some of the newest insights into this phenomenon.

For these types of objects, studies in the near-IR are particularly profitable. This is primarily due to the low dust opacity, the low contamination from molecular lines, and the high luminosity of the sources. As well as resolving the structure of the circumstellar material, our observations have also yielded information on numerous stellar properties such as pulsational modes, atmospheric structure, giant convective cells and the overall photospheric symmetry of evolved stars.

2. EXPERIMENTAL DESIGN

Unlike conventional aperture masking experiments, which use screens in a re-imaged pupil plane, masking of the Keck 1 primary was achieved by mounting custom-made plates in front of the f/25 secondary mirror. The masks were designed with the aid of the CODE V optical ray-trace package, which allowed us to take account of complications arising from this location in the optical train, most notably the double light path through the masks, and the effects of the converging beam. A surprising advantage of the mask location in the secondary mirror top-end assembly was that by driving the telescope to the horizon, the masks could be accessed and changed from the Nasmyth deck of the Keck telescope in the night by the observers.

Figure 1 shows a typical 15-hole mask in projection on the Keck primary mirror. In general, many constraints need to be satisfied before arriving at such pupil geometries, the primary concern being to sample the Fourier plane evenly and densely out to the cut-off of the telescope with a *non-redundant* array. Our designs are generalizations of those of Golay (1970), who searched 3-fold symmetric parameter spaces for optimally compact arrays satisfying the condition for non-redundancy; i.e. that no vector baseline occurs more than once. In our case, this search process was greatly complicated by the need to fit the array into the Keck telescope pupil while avoiding sampling across the cracks between segments, and blockage by the spiders and undersized secondary.

After passing through the mask (twice), starlight was bought to focus in the Near Infra-Red Camera (NIRC), a cryogenically cooled 256×256 pixel InSb array (Matthews & Soifer 1994). Using the NIRC magnifying optics (Matthews et al. 1996) gave a pixel scale of 20.57 milli-arcsec/pixel – sufficient to Nyquist sample fringes on the longest baselines in K-band. While we would have preferred to use a continuously variable narrow-band filter, NIRC has no such facility, and so observations were secured using the existing filterset between 1.0 and 3.3 μm. Unfortunately, technical difficulties were encountered at both extremes of this range.

At long wavelengths, the thermal background from the sky and telescope rapidly becomes significant, and neccessitates the use of very short exposure times to avoid saturation of the camera. With an ambient-temperature mask occupying most of the pupil, this problem is greatly exacerbated. We were able to obtain excellent data at 3.3 μ by sub-framing the array to obtain rapid exposure times, but the lack of a cold mask internal to the camera precluded opereration at still longer wavelengths.

At wavelengths shorter than 2 μm, the 20.57 milli-arcsec/pixel plate scale was no longer sufficient to Nyquist sample the interference fringes on the longest baselines. If observations are made, power on such baselines is "aliased" back into the power spectrum at lower spatial frequencies, and in most experiments, this signal will overlap and become confused with other shorter baseline signals. However, for sparse pupils these aliased baselines can often correspond to otherwise unmeasured spatial frequencies, and so the measurements on these aliased baselines remain possible. In practice, however, the undersampling of the data attenuates the signals significantly and makes the recovery of good data possible in only a handful of cases where the fringes are very strong. Nevertheless, we have used this device to recover the J band visibility functions of a small number of the brightest supergiants and Miras beyond their first nulls.

To accommodate a range of source brightnesses and maintain good fourier plane coverage we have relied upon a range of pupil masks, which can be swapped during the night with little penalty in time. In addition to the non-redundant arrays described above, observations have also been made with annulus-shaped pupils such as that depicted in Figure 1 (see Haniff & Buscher 1992), and with the fully-filled aperture (FFA). Typically the non-redundant arrays were used to obtain the highest SNR data on bright stars, while partially-redundant or FFA geometries were selected to optimize the observations of dimmer stars.

In common with most high-resolution interferometric experiments, it was necessary to use the shortest possible integration times to "freeze" the atmospheric seeing. Ideally the integration time should have been less than the atmospheric coherence time (~50 msec at 2.2 μm), however limitations in the chip readout electronics dictated integration times typically around 100 to 150 msec. Although this was not optimal, we were still able to recover information on the finest spatial scales from such speckle frames.

3. DATA REDUCTION

Figure 2 shows a typical short-exposure interferogram detected at the infrared array. The geometric pattern results from the Airy disks of the small circular sub-apertures being crossed by numerous (105 in this case) fringe patterns arising from interference between each pair of holes in the mask. The contributions from each baseline can be separated and measured by taking the power spectrum of sequences of such images, as shown to the right, where we have accumulated the mean spectrum over 100 separate interferograms. It is interesting to note that this illustrates the Fourier coverage afforded by the array, and in this case the sampling out to the limit of the 10 m pupil is extremely good.

As is normal, our data reduction proceeded by extracting the visibilities and phases from each short-exposure. Such data are related to the brightness distribution of the science target by a Fourier transform (e.g. Born &

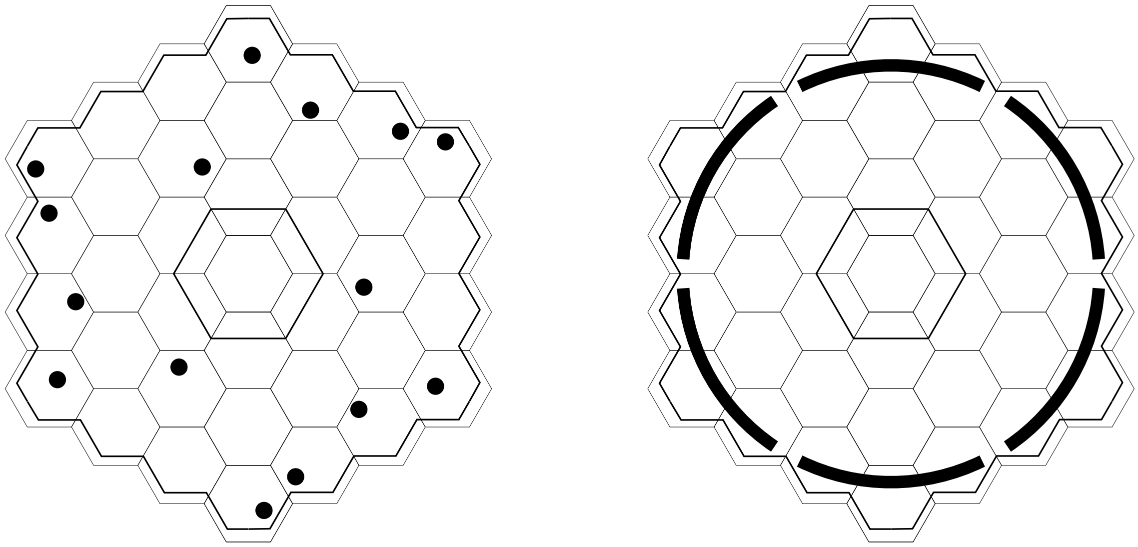

Figure 1. Examples of some of the pupil geometries used for our Keck masking experiment. A 15-hole non-redundant array (left) and an annulus mask (right) are shown superimposed over scaled images of the Keck primary mirror.

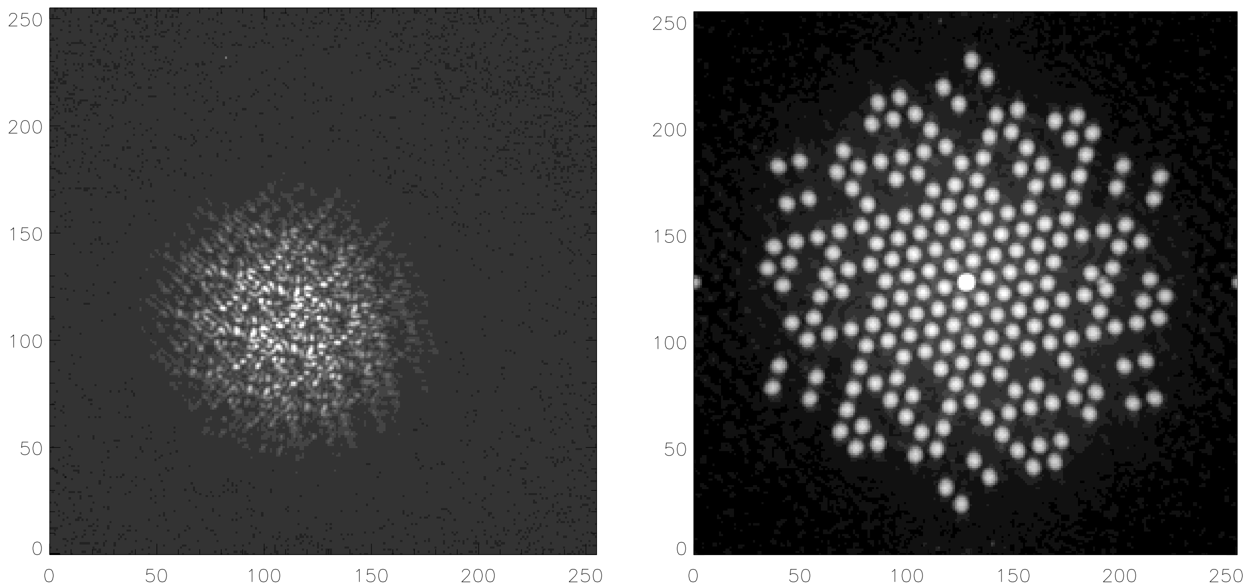

Figure 2. Interferogram of a point-source star taken at $2.2\,\mu$m (left) through the 15-hole non-redundant mask depicted in Figure 1. The right hand panel is the result of accumulating the power spectra of 100 such raw data frames.

Wolf 1964). Although the Fourier phases are corrupted by atmospheric phase fluctuations, an observable known as the *closure phase* – the sum of baseline phases around closed triangles – has been developed in radio astronomy to overcome this problem. These techniques are now well established at optical wavelengths (Haniff et al. 1987, Roddier 1988).

The raw Fourier data were calibrated for the mean telescope–atmosphere transfer function by utilizing nearly contemporaneous observations of point-source stars. Our observing regimen devoted an equal amount of time to such calibration stars, interleaving observations of them with those of the science targets under nearly-identical conditions. Even so, seeing and other changes make this calibration process notoriously difficult and mismatches between source and calibrator data introduced the greatest uncertainty into our final results.

Having obtained a set of calibrated visibilities and closure phases, images were recovered from these data using a number of mature algorithms developed for similar radio astronomcial applications, i.e. the recovery of images from noisy and sparseley sampled fourier data. For the results presented here we have used one of the most popular of these, known as the "Maximum Entropy Method" (Gull & Skilling 1984, Sivia 1987). In order to check the reliability of our results we have compared our mem reconstructions with those obtained using the CLEAN reconstruction algorithm (Högbom 1974), also used widely in radio astronomy. In some cases, quantitative information was also extracted by fitting models directly to the Fourier data.

It is interesting to note that under typical conditions a very small number of speckle frames could be used to reconstruct a reliable diffraction-limited map. A single set of 100 source frames, paired with an additional 100 point-calibrator frames, taking perhaps 5 min of telescope time to secure (including overheads), was often sufficient to produce an excellent monochromatic image of one of our science targets. This efficiency results from the key feature of aperture masking, i.e. that extremely high signal-to-noise visibility data can be obtained from a very small number of interferograms.

A demonstration of the signal-to-noise advantages obtained when the pupil is transformed from fully redundant, to partially redundant, and finally to a non-redundant geometry is presented in Figure 3. For the visibility data, the principle effect of decreased redundancy has been to make the visibilities of a point-source calibrated with a second point source all closer to 1.0. For the other pupils, changes in the seeing while moving the telescope between the stars has affected the data, resulting in a mis-calibration. Interference patterns generated by the non-redundant pupil are more stable against such seeing changes, and are thus easier to calibrate reliably. For the closure phases, data extracted from observations with the Golay mask show a spread of only a few degrees around the expected value of 0°. Atmospheric noise, which plays an increasing role as the pupil is made partially then fully redundant, degrades the closure phase data for the other masks, and leads to much larger closure errors.

4. RESULTS

One astrophysical area that we have focussed on concerns long-period variables. For these stars, an outstanding problem has been the precise determination of their angular diameters (Wood 1990). This has important repercussions for stellar dynamical modeling: precise diameter measurements coupled with good distance estimates provide the most direct method of determining the mode of stellar pulsation. In the past interferometric observations at optical wavelengths have been complicated because the stellar spectrum is blanketed by molecular lines formed in intermediate layers above the continuum photosphere (Scholz & Takeda 1987). Measurements in the mid-IR are similarly contaminated by emission from circumstellar dust. The near-IR offers thus the best hope for measuring the stellar photosphere.

Our diffraction-limited observations with the Keck telescope have enabled us to measure photospheric stellar diameters in a number of near-IR wavebands, as illustrated in Figure 4. These data allowed us to address a number of important topics in the study of evolved stars:

1. When combined with distance estimates for a sample of stars (e.g. from Hipparcos), dynamical studies, such as those of Haniff et al. (1995), can determine the pulsation mode and other fundamental dynamical properties.

2. Quasi-monochromatic diameters at a range of wavelengths probe the atmospheric structure, helping to discriminate emission from the photosphere, molecular atmosphere and circumstellar dust, thereby providing valuable experimental testing of numerical model atmospheres.

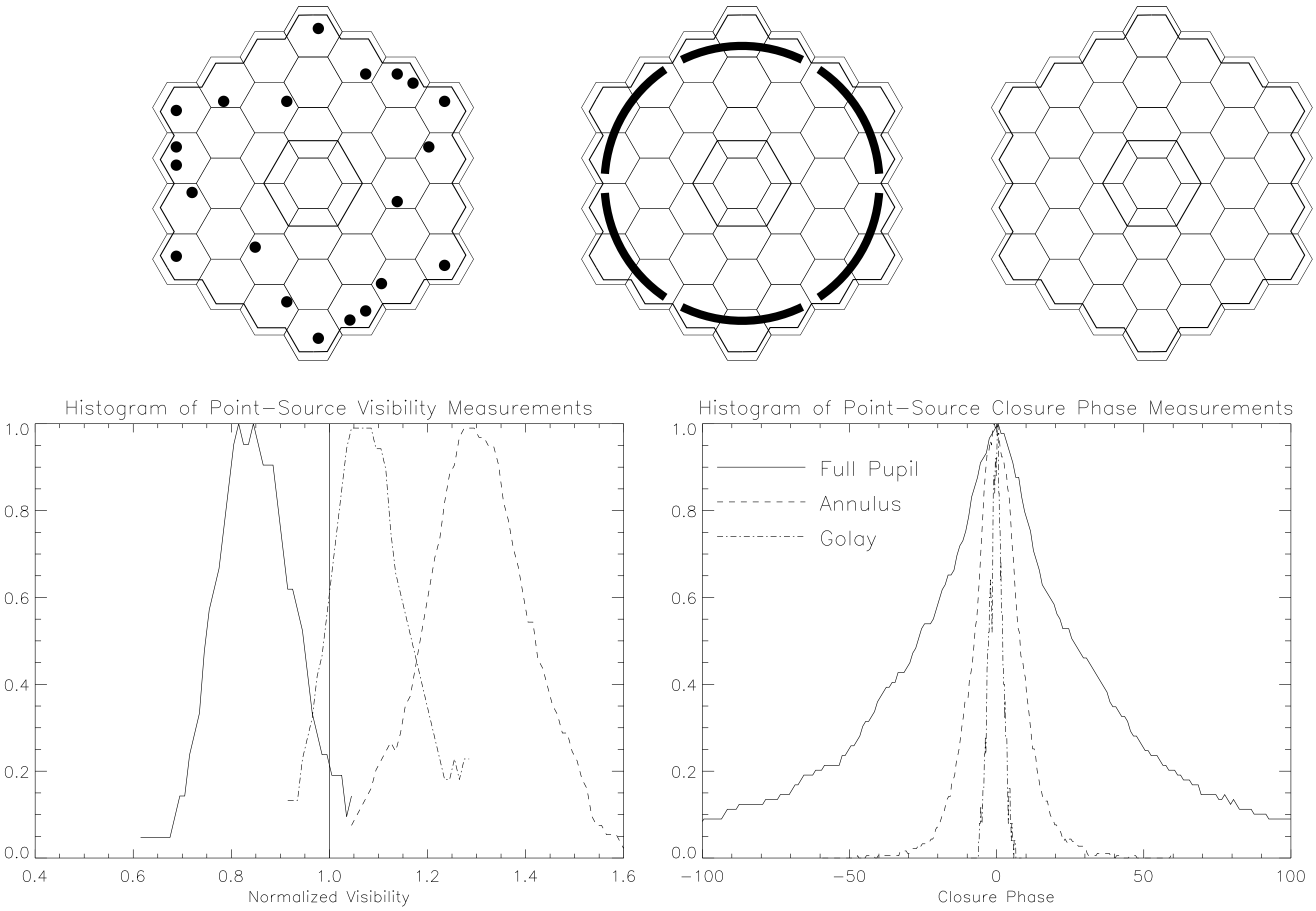

Figure 3. A comparison of complex visibility data taken with a 21-hole non-redundant Golay mask (top left), an annulus mask (top center) and with the full unobstructed pupil (top right). Observations were made of an unresolved point-source star which should yield visibility amplitudes of 1.0, and closure phases of 0.0. A histogram of calibrated visibilities (left) shows that the Golay mask data shows values closest to 1.0 - indicating that the calibration process has proved most reliable for this data. More dramatically, the histogram of values of the closure phase (right) shows the extremely narrow scatter (about 5°) about zero obtained with the non-redundant mask, as compared with the increasingly broad distributions from masks with greater redundancy.

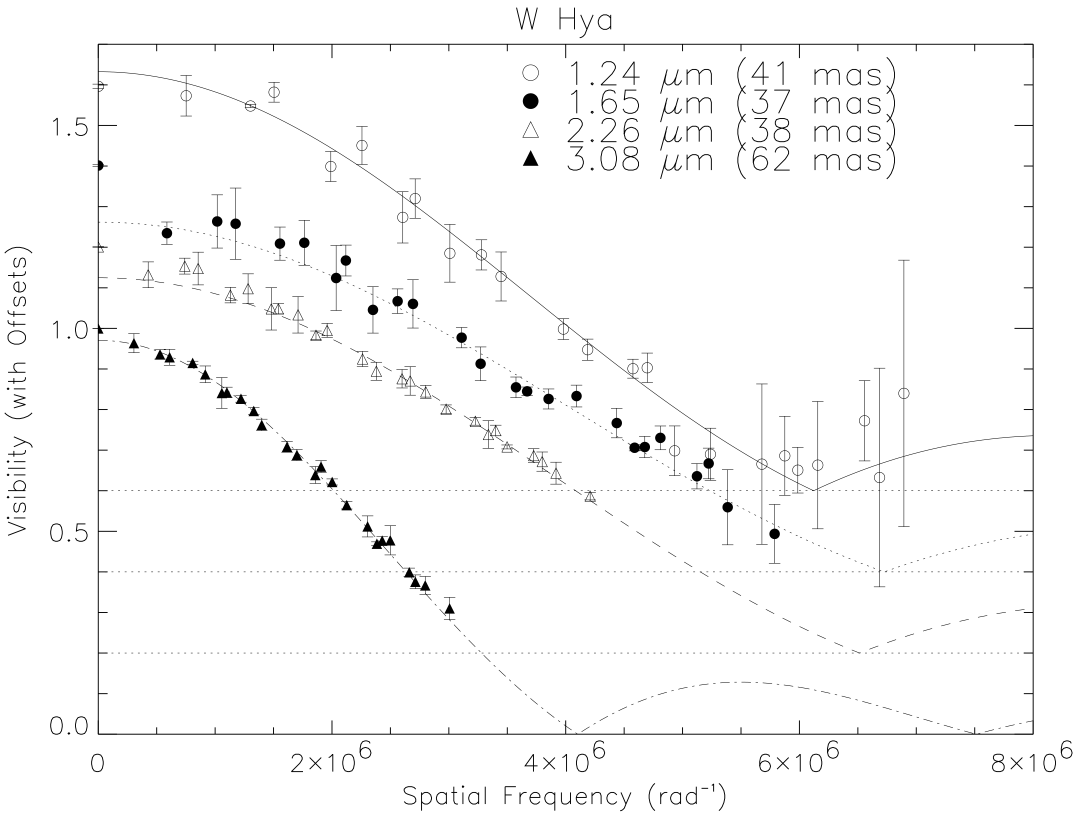

Figure 4. Azimuthally averaged visibility curves produced for W Hya from multi-wavelength speckle data. Diameters given correspond to the best-fit uniform-disk models, which can be seen to be well matched to the data. The larger apparent diameter recorded at $3.08\,\mu$m is probably due to molecular or dust blanketing around the star.

3. Time-series measurements of stellar diameters through the pulsation cycle should be able to directly observe changes in the photospheric radius.

4. Bright asymmetric features, or hotspots, have been detected on the surfaces of late-type stars (Buscher et al. 1990, Tuthill et al. 1997, Gilliland & Dupree 1997), while other workers have reported elliptical distortions of the photosphere (Karovska et al. 1991, Quirrenbach et al. 1992). Our measurements provide images at the highest resolution yet in the near-IR, and can thus help to identify the physical mechancisms responsible for such features.

As well as studying the stellar photosphere, some of our target sources possess dusty circumstellar halos. At the diffraction limit of the Keck telescope, we have been able to resolve these shells for some of the most well-studied, prototypical evolved stars. Spectacular images showing shells, clumps and outflows have been obtained for IRC +10216, CIT 6, NML Cyg and VY CMa. To give a flavor of this work within the constraints of this report, we focus here on the red supergiant VY CMa.

Although optical nebulosity around VY CMa has been known for most of this century, it was not until the imaging polarimetry of Herbig (1972) that bright knots within this structure were revealed as scattering enhancements rather than companion stars as had previously thought. More recently, HST/FOC imaging (Kastner 1997) of the visible halo has revealed not only the well-known $\sim$3 arcsec extension to the west, but also a complex and dynamic inner region.

The dust formation zone close to the star is best viewed at infrared wavelengths due to the high scattering-induced optical depths in the visible. Figure 5 shows our keck images of VY CMa's bright inner the dust envelope at 2.2 and

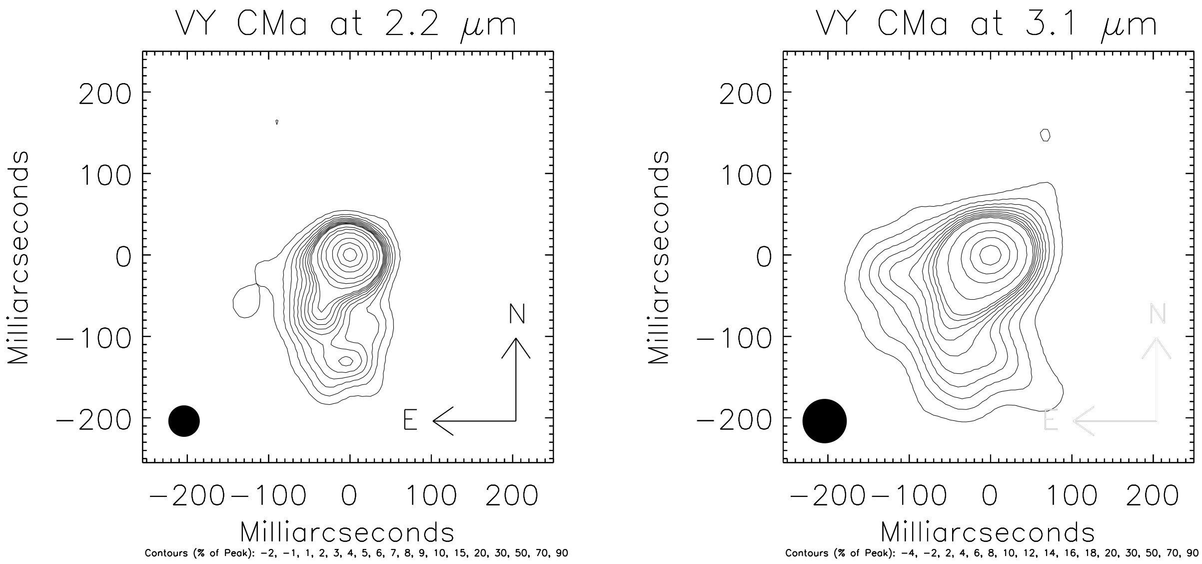

Figure 5. Maps of the supergiant VY CMa at 2.2 and 3.1 μm reconstructed from aperture synthesis imaging data. Contours are 2,4,6,8,10,20,50 and 90 % of the peak.

3.1 μm. The extremely high spatial resolution achieved with the keck has revealed asymmetric, one-sided thermal emission to the south with a slight spiral structure. This emission is almost certainly a tracer for a dust clump or outflow whose proximity to the photosphere makes it hot enough to radiate in the near-IR.

For many of our targets, there is is evidence for asymmetry in the mass-loss process from polarization studies (Trammel et al. 1994), molecular data, the fitting of spherically-symmetric broad-band spectro-photometric models (e.g. Planesas et al. 1990) and VLBI mapping of maser emission (e.g. Greenhill et al. 1995). However, it has never been possible to image the circumstellar dust surrounding these stars at sufficiently high resolution to infer the details of these asymmetries. Our program with the Keck has demonstrated the ability to resolve the hot dust emission on small scales, revealing unambiguous signatures of anisotropic mass-loss close to the stellar surface. This raises intriguing questions as to why mass loss seems to be a fairly spherically symmetrical process in some stars yet not in others. Could this be related to binarity, stellar rotation, or perhaps some other stellar property? Clearly futher observations at high angular resolution hold the key.

ACKNOWLEDGMENTS

We would like to thank Devinder Sivia for the maximum-entropy mapping program "VLBMEM" which we have used to reconstruct our diffraction-limited images. We would also like to thank Everett Lipman, Ed Wishnow, Charles Townes, Peter Gillingham and Terry McDonald for help in various ways. This work has been supported by grants from the National Science Foundation (AST-9321289 and AST-9315485) and the Office of Naval Research (N00014-93-0775 and N00014-96-1-0737).

REFERENCES

1. Born M. & Wolf E. 1964, *Principles of Optics*, Macmillan, New York.
2. Buscher D.F., Baldwin J.E., Warner P.J. & Haniff C.A. 1990 *Mon. Not. R. ast. Soc.*, **245**, 7B
3. Gilliland R.L. & Dupree A.K. 1997, *Astrophys. J.*, **463**, L29
4. Golay M. 1971, *J. Opt. Soc. Am.*, **61**, 272
5. Greenhill L.J., Colomer F., Moran J.M., Backer D.C., Danchi W.C., & Bester M. 1995, *Astrophys. J.*, **449**, 365.
6. Gull S.F. & Skilling J. 1984, *IEEE Proceedings*, **131**, Pt. F, No.6

7. Hale D., Bester M., Danchi W.C., Hoss S., Johnson M., Lipman E.A., Lopez B., Monnier J.D., Tuthill P.G., Geballe T.R., and Townes C.H. 1997 *Astrophys. J.*, **490**, 407
8. Haniff C.A., Mackay C.D., Titterington D.J., Sivia D., Baldwin J.E. & Warner P.J. 1987, *Nature*, **328**, 694
9. Haniff C.A. & Buscher D.F. 1992, *J. Opt. Soc. Am., A*, **9**, 203
10. Haniff C.A., Scholz M. & Tuthill P.G. 1995, *Mon. Not. R. ast. Soc.*, **266**, 745
11. Herbig G.H. 1972, *Astrophys. J.*, **172**, 375
12. Högbom J. 1974 *Astrophys. J. Suppl.*, **15**, 417
13. Karovska M., Nisenson P., Papaliolios C., Boyle R.P. 1991, *Astrophys. J.*, **374**, L 51
14. Kastner J.H., 1997 *Hubble Archive*, proposal GO-6416
15. Matthews K, & Soifer B.T. 1994, *Astrophys. & Space Science*, **190** 239
16. Matthews K, Ghez, A. M., Weinberger, A. J. & Neugebauer G. 1994, *PASP*, **108** 615
17. Planesas P., Kenney J., Bachiller R. 1990, *Astrophys. J.*, **364**, L9
18. Quirrenbach A., Mozurkewich D., Armstrong J.T., Johnston K.J., Colavita M.M. & Shao M. 1992, *Astr. Astrophys.*, **259** L19
19. Roddier F. 1988, *Physics Reports*, **170**, 97
20. Scholz M. & Takeda Y. 1987, *Astr. Astrophys.*, **186**, 200
21. Sivia D.S. 1987, *Ph.D. Dissertation*, Cambridge University
22. Trammel S.R., Dinerstein H.L. and Goodrich R.W. 1994, *Astron. J.*, **108**, 984
23. Tuthill P.G., Haniff C.A. & Baldwin J.E. 1997, *Mon. Not. R. ast. Soc.*, **285** 529
24. Wood P.R. 1990, in Mennessier M.O. & Omont A., (eds) Editions Frontières, Gif-sur-Yvette, P.67